BULETINUL INSTITUTULUI POLITEHNIC DIN IAŞI
Publicat de
Universitatea Tehnică „Gheorghe Asachi” din Iaşi
Volumul 68 (72), Numărul 4, 2022
Secţia
CONSTRUCŢII DE MAŞINI
DOI:10.2478/bipcm-2022-0037

A STUDY ON THE SYNTHESIS OF 2D PROFILES FOR CYCLOIDAL DISCS USED IN CYCLOIDAL REDUCERS

BY

MIHĂIŢĂ HORODINCĂ*, EDUARD NECULAI BUMBU, ADRIANA MUNTEANU, DRAGOŞ FLORIN CHITARIU and FLORIN CHIFAN

“Gheorghe Asachi” Technical University of Iaşi,
Faculty of Machine Manufacturing and Industrial Management

Received: December 22, 2022
Accepted for publication: December 28, 2022

Abstract. This paper proposes a simple approach on the synthesis of the 2D profiles for the rotors of cycloidal reducers. A 2D rotor (or cycloidal disc) profile (as a complex closed curve) can be defined (as an alternative to the strictly mathematical definition) as the internal bordered envelope of the family of 2D profiles of the stator (or ring gear) obtained with the stator movable (for at least a completely rotation) around the fixed rotor (or planetary gear) by respecting the gearing conditions inside a cycloidal reducer. The more 2D profiles of the stator are used the more accurate definition of 2D rotor profile is obtained. The finding of *x*, and *y*-coordinates of the points involved in the description of this 2D rotor profile is by far the most complicated problem to solve in the manufacturing of this type of reducer, the behavior and performances of the cycloidal reducer drastically depends by the accuracy of this profile. The results of this study can be easy applied in practice.

Keywords: Cycloidal reducer, rotor, cycloidal disc, 2D profile, computer aided synthesis.

*Corresponding author; *e-mail*: horodinca@tuiasi.ro.
© 2022 Mihăiță Horodincă et al.
This is an open access article licensed under the Creative Commons Attribution-NonCommercial-NoDerivatives 4.0 International License (CC BY-NC-ND 4.0).

1. Introduction

A cycloidal reducer (CR, or cycloidal drive or cycloidal gear) is well known in the literature, being used frequently to drive rotary machines and mechanisms. It provides low gear ratio values, high torque and presents a simple, robust and compact design, as an alternative of many other types of gear reducers (*e.g.* a planetary reducer). In fact a CR is as a particularly case of a planetary reducer, which does not have a sun gear. An input rotor having Z_R teeth (or lobes) rotates (using a carrier) as a planet gear, being in gear with a fixed stator (ring gear) where $Z_S=Z_R+1$ equidistant teeth (as cylindrical shape pins) are placed. The input motion is the rotation of a carrier or the rotation of rotor center around the center of the ring gear as well. The output motion is the rotation of the rotor around its (rotary) center. The access to the output motion is a critical issue to solve in a CR design. This relative big disadvantage of CR is fully compensated by some important advantages. The first advantage is the small value of the gear ratio ($-1/Z_R$). The second advantage is the possibility to replace the fixed cylindrical pins placed as gear teeth on the ring gear (CR stator) by rotary pins or bearings. This practically happens in all modern designs of CR. This way the severe internal friction between rotor and stator teeth is drastically reduced, the CR power efficiency increases a lot, with less noise during operation. Now CR acts as a gear reducer with sliding friction replaced by rolling friction.

Because this particularity of CR (cylindrical shape pins used as teeth on the fixed ring gear) the rotor should have a special external shape in order to respect strictly the gearing law. This external shape of the rotor in a transverse section is a 2D profile similarly to a curtate closed epicycloid with Z_R lobes. That is why the rotor is also currently named cycloidal disc, or rarely epitrochoid disc in (Huang and Tsai, 2017).

There are some studies focused on this critical topic, most of them focused on the mathematical description of the 2D cycloidal disc transverse section (profile). In 2006 (Shin and Kwon, 2006) proposes a parametrical description of this profile, used later on for different researches involved in CR power efficiency studies (Wang *et. al.*, 2019; Allota *et al.*, 2021; Mackic, 2013) and contact forces distribution in (Huang and Tsai, 2017). Similarly (Petrovic *et al.*, 2013) proposes a mathematical description and a computer program useful to generate this profile (called also shortened equidistant epitrochoid curve) for different CR parameters. Some achievements proposed by (Litvin and Feng, 1996) related to a theoretical approach of the cycloidal gears profiles used in Wankel engine, Root's blowers and pumps are also useful as referential paper for this work.

The main objective of this paper is to propose an alternative method to obtain a description of the external shape of the CR cycloidal disc through the

coordinates of the points involved in its 2D transverse section description, in a Cartesian coordinate system.

This transverse section (2D profile) can be described as an internal envelope of a family of epicycloid curves generated by all the points of all the pins from the stator when the stator moves related to a fixed rotor. This is another reason why the CR rotor is currently named cycloidal disc.

There is a simpler method proposed and validated in this paper in describing the 2D cycloidal disc profile (as the result of the simulation of the CR operation) in a particular way: as the internal envelope of the family of stator (ring gear) positions related to the fixed rotor (cycloidal disc). Two main objectives are accomplished in this paper: first is the generation of this family of stator positions, second is the detection of description of the internal envelope of this family of stator positions. This method assures a safely and precise definition of 2D cycloidal disc profile. This method was already partially introduced in a previous work focused on sine-gear 2D profiles description used in internal cylindrical gears manufacturing (Horodincă, 2020).

Section 2 of this paper focuses on a theoretical approach on the geometrical description of the positions of the movable stator related to the fixed rotor. Section 3 presents some results on simulations of these positions. Section 4 focuses on the detection of the coordinates of internal envelope of these positions. Section 5 presents a way to transfer the 2D cycloidal disc profile on the external shape of the cycloidal disc, with an example on a CAD model. Section 6 presents the conclusions and the future work.

2. A theoretical approach on the stator (ring gear) motion relative to the rotor (cycloidal disc)

The generation of the family of the mobile stator 2D profiles (the stator as ring gear, also called pins housing or fixed ring, having Z_S pins) related to the (fixed) rotor (as planet gear, also called cycloidal disc or rolling disc, having Z_R teeth) is based on a theoretical approach exposed here below.

Figure 1 presents some considerations on the cycloidal reducer (CR) working principle and gear ratio calculus.

The planet gear (the CR rotor) is firmly attached to the circle (R) having radius r_R. The circle (R) is the rolling circle of the rotor (having the center in O_2). The ring gear (the CR stator) is firmly attached to the circle (S) having radius r_S. The circle (S) is the rolling circle of the stator (having the center in O_1). These circles are permanently tangents in a movable point P_t. The stator is fixed (the circle (S) does not rotate around its center O_1) while the rotor has simultaneously two strictly correlated rotary motions: the counterclockwise (CCW) rotation of the center O_2 around the center O_1 with $n_{O_2-O_1}$ a (fast) rotary speed (as input motion in CR) and the clockwise (CW) rotation of the rotor (and

the circle (R) as well) around its center O_2 with n_{R-O_2} a (slow) rotary speed (as output motion in CR).

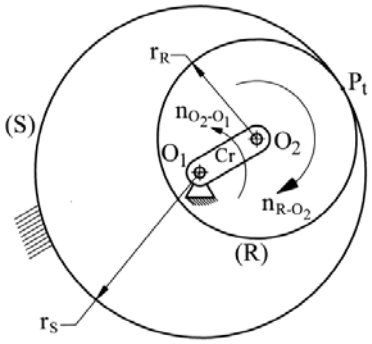


Fig. 1 – A sketch on cycloidal reducer working principle.

The input motion is introduced by a crank Cr (also called carrier) which rotates around the fixed center O_1 while the output motion (a rotary motion around a rotary point O_2) is taken by a relatively complicated mechanical system, because the rotary output motion should be mandatory around a fixed axis (point). The use of this system is one of the main disadvantages of CR (the other one is the mechanical unbalance of the rotor). The length l_{Cr} of the crank or the cycloidal disc eccentricity, or the distance $d_{O_2-O_1}$ between centers as well should be mandatory described as: $d_{O_2-O_1} = l_{Cr} = r_S - r_R$.

Taken into account that the CR output and input motions are in opposite directions (as indicated in Fig. 1) and Z_S - Z_R=1, the gear ratio of CR is described by a known relationship (neglecting the behaviour as reverse reducer):

$$\frac{n_{R-O_2}}{n_{O_2-O_1}} = \frac{r_S - r_R}{r_R} = \frac{Z_S - Z_R}{Z_R} = \frac{1}{Z_R} \tag{1}$$

There is available a first equivalent CR working principle (already used before in Horodincă and Seghedin, 1996) which is noticeable for an observer placed in the center of rotation O_2, briefly described in Fig. 2.

For this observer, the circle (R) rotates CW (with the output motion of CR) around its fixed center O_2 with the rotary speed n_{R-O_2} while the circle (S) has a special kind of motion: each point of this circle (and of course its center O_1) has a circular motion, it moves CCW around a circle with fixed center and radius $d_{O_2-O_1}$. This motion is provided by a simple mechanism, based on (at least) three strictly parallel cranks $Cr_{1\div3}$ having rigorously the same length $l_{Cr_{1\div3}} = d_{O_2-O_1}$ which rotate simultaneously with the same rotary speed ($n_{O_1-O_2}$) around its fixed revolute joints (O_3, O_4 and O_5). One crank is active, the other two are passive. At the other end of each crank there is another revolute joint (O_6, O_7 and O_8) with the circle (S). In each of these last revolute

joints the parent link is attached to the crank while the child link is attached at circle (S).

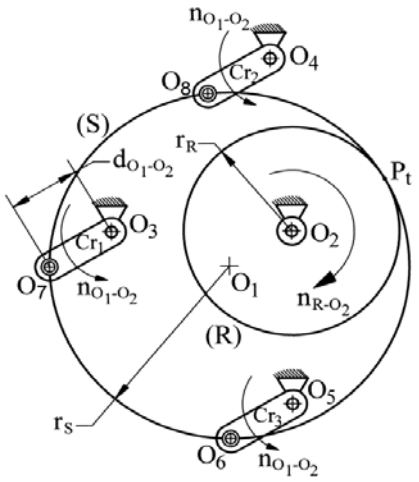


Fig. 2 – A sketch on a first equivalent cycloidal reducer working principle.

We use the notation of rotary speed $n_{O_1-O_2}$ (of the input motion in CR applied around the fixed revolute joint at one of cranks Cr_i) because now the center O_1 rotates around the center O_2 with this speed. Of course $n_{O_1-O_2}$ here from Fig. 2 has strictly the same value and direction with $n_{O_2-O_1}$ (from Fig. 1). Of course this first equivalent cycloidal reducer assures the same value for gear ratio, already given before in Eq. (1), also with output motion in opposite direction related by input motion (here CW versus CCW).

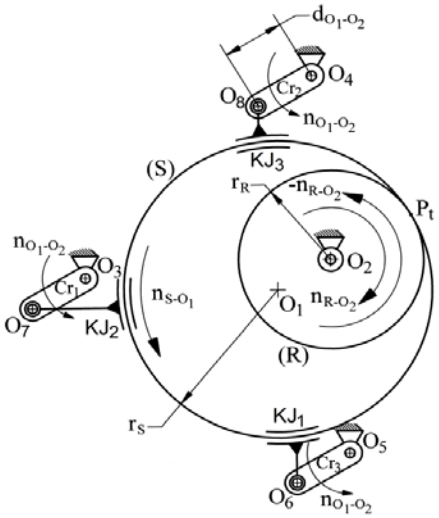


Fig. 3 – A sketch on a second equivalent cycloidal reducer working principle.

There is available a second equivalent CR working principle (probably useless for a future design, but very useful for our theoretical approach), as described in Fig. 3.

Suppose now that in the same working conditions exposed in Fig. 2 we should rotate in CCW the circle (R) around its fixed center O_2 exactly with n_{R-O_2} rotary speed. This is possible only if -according with Fig. 3- we accept that the circle (S) is free to rotate CCW around its center O_1 on three conceptual kinematic joints $KJ_{1\div3}$, each one attached at the child link of $O_{6\div8}$ revolute joints. Now the circle (R) and its center is fixed but because of the CCW rotation previously introduced, and because the circles (R) and (S) acts as internal rolling circles, the circle (S) should mandatory rotates also CCW with n_{S-O_1} rotary speed expressed in the internal gear ratio:

$$\frac{n_{s-O_1}}{n_{R-O_2}} = \frac{r_R}{r_s} = \frac{Z_R}{Z_S} \tag{2}$$

Now inside the second equivalent CR (Fig. 3) it happen two implications. Firstly the CCW input motion $n_{O_1-O_2}$ (equal with $n_{O_2-O_1}$ from Eq. (1)) implies the CW n_{R-O_2} motion defined (from Eq. (1)) as:

$$n_{R-O_2} = n_{O_2-O_1} \cdot \frac{r_S - r_R}{r_R} = n_{O_2-O_1} \cdot \frac{Z_S - Z_R}{Z_R} = n_{O_2-O_1} \cdot \frac{1}{Z_R} \tag{3}$$

Secondly the CCW motion n_{R-O_2} necessary to make fixed (unmovable) the circle (R) implies the CCW output n_{S-O_1} rotary motion established from Eq. (2) as:

$$n_{s-O_1} = n_{R-O_2} \cdot \frac{r_R}{r_s} = n_{R-O_2} \cdot \frac{Z_R}{Z_S} \tag{4}$$

With n_{R-O_2} from Eq. (3) placed in Eq. (4), the output motion n_{S-O_1} gets the value:

$$n_{s-O_1} = n_{O_2-O_1} \cdot \frac{r_S - r_R}{\cancel{r_R}} \cdot \frac{\cancel{r_R}}{r_s} = n_{O_2-O_1} \cdot \frac{Z_S - Z_R}{\cancel{Z_R}} \cdot \frac{\cancel{Z_R}}{Z_S} = n_{R-O_2} \cdot \frac{\cancel{Z_R}}{Z_S} \cdot \frac{1}{\cancel{Z_R}} \tag{5}$$

From Eq. (5), if Z_S - Z_R=1 (typically for a CR), the gear ratio of the second equivalent CR becomes:

$$\frac{n_{s-O_1}}{n_{O_2-O_1}} = \frac{r_S - r_R}{r_s} = \frac{Z_S - Z_R}{Z_S} = \frac{1}{Z_S} \tag{6}$$

An important consequence results from Eq. (6). If the center O_1 rotates around the center O_2 with an angle α in a certain direction (starting from an angular origin) than the circle (S) rotates around its center (O_1) with an angle β

(starting from an angular origin) in the same direction. The ratio β/α between these angles is obviously equal with the ratio between rotary speeds given by Eq. (6) or with the gear ratio of the second equivalent CR as follows:

$$\frac{\beta}{\alpha} = \frac{n_{s-O_1}}{n_{O_2-O_1}} = \frac{r_S - r_R}{r_s} = \frac{Z_S - Z_R}{Z_S} = \frac{1}{Z_S} \tag{7}$$

The Eq. (7) can be rewritten as:

$$\beta = \alpha \cdot \frac{r_S - r_R}{r_s} = \alpha \cdot \frac{Z_S - Z_R}{Z_S} = \alpha \cdot \frac{1}{Z_S} \quad \text{or} \quad \beta Z_S = \alpha \tag{8}$$

It is important to highlight here the mandatory relationship between the radii r_S and r_R in CR design: with $r_S/(r_S - r_R)=Z_S$ (from Eq. (6) and $r_R/(r_S-r_R)=Z_R$ (from Eq. (3). In other words the ratios $r_S/(r_S-r_R)$ and $r_R/(r_S-r_R)$ should be positive integers. Because in a CR $Z_S - Z_R=1$, it follows that is mandatory to have:

$$\frac{r_S}{r_S - r_R} - \frac{r_R}{r_S - r_R} = 1 \tag{9}$$

In order to generate and to draw the family of the stator 2D profiles, it is necessary to know the coordinates x_{Sm}, y_{Sm} of the points of stator 2D profile (ring gear) in a first (mobile) Cartesian coordinates system (as MCCS) with the origin in the center of rolling center or the ring gear (O_1). This profile should be placed with the center in the point O_1 (Fig. 3). A position of the stator 2D profile related to the rotor (cycloidal disc) is completely characterized by the angles α and β. The relationship between α and β is described in Eq. (8), as $\beta= \alpha/Z_S$. In order to generate a position (α, β) of the stator in a second (fixed) Cartesian coordinates system (as FCCS, with the origin in O_2) firstly the center O_1 (placed at the distance r_S-r_R from the point O_2) together with the stator 2D profile must be rotated with the angle α around the center O_2. Secondly the stator 2D profile must be rotated around the center O_1 in the same direction together with MCCS, with the angle β. Of course the succession of the two rotations can be changed.

With these comments, the abscissa x_{Sf} of a point of stator 2D profile (ring gear) in the FCCS for a position (α, $\beta=\alpha/Z_S$) can be calculated as:

$$x_{Sf}(\alpha) = (r_S - r_R) \cdot \cos(\alpha) + x_{Sm} \cdot \cos\left(\frac{\alpha}{Z_S}\right) - y_{Sm} \cdot \sin\left(\frac{\alpha}{Z_S}\right) \tag{10}$$

The first term in the right-hand side of Eq. (10) describes the projection on x-axis of FCCS for the distance (r_S-r_R) between O_2 and O_1, supposing that the origin of the angle α is this x-axis. The second and the third term describes together the projection of the point x_{Sm}, y_{Sm} of stator 2D profile from rotated MCCS (with angle $\beta=\alpha/Z_S$) on x-axis of FCCS.

Similarly, the ordinate y_{Sf} of a point of stator 2D profile (ring gear) in the FCCS for a position (α, $\beta=\alpha/Z_S$) can be calculated as:

$$y_{Sf}(\alpha) = (r_S - r_R) \cdot \sin(\alpha) + y_{Sm} \cdot \cos\left(\frac{\alpha}{Z_S}\right) + x_{Sm} \cdot \sin\left(\frac{\alpha}{Z_S}\right) \qquad (11)$$

The first term in the right-hand side of the Eq. (11) describes the projection on y-axis of FCCS for the distance (r_S-r_R) between O_2 and O_1, The second and the third term describes together the projection of the point x_{Sm}, y_{Sm} of stator 2D profile from rotated MCCS (with angle $\beta=\alpha/Z_S$) on y-axis of FCCS.

3. An approach on the simulation of stator (ring gear) positions relative to the rotor (cycloidal disc)

Some simulations were done using Matlab in order to validate the previous theoretical approaches. The first validation of Eq. (10) and (11) is described in Fig. 4. Here with magenta colour are depicted some successive positions of a single 2D circular pin profile (placed as a gear tooth on a ring gear, with $Z_S=15$) having the radius $r_p=9.8257$ *mm*, related to a fixed cycloidal disc (with $Z_R=14$) for the CCW evolution of angle α between 0 and 2π in a conceptual CR (with $r_S=94$ *mm*, $r_R=87.7333$ *mm* with the center of this pin profile placed on a circle with radius $r_{pp}=r_S$). Each two successive positions are obtained with an incremental variation $\Delta\alpha = 2\pi/50$ for the angle α. A position of this pin is highlighted in red.

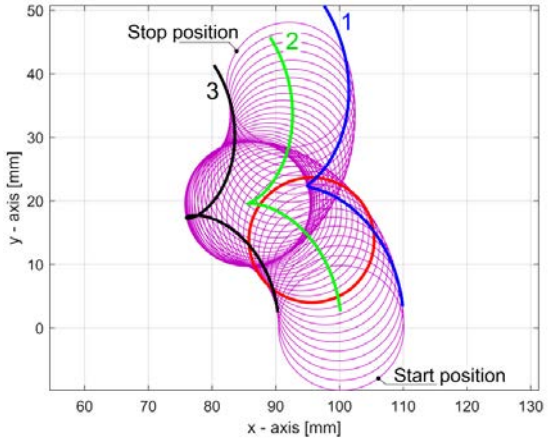


Fig. 4 – Some successive positions of a circular 2D pin profile placed as a gear tooth on the ring gear, related to a fixed cycloidal disc, for an incremental variation $\Delta\alpha = 2\pi/50$ of the angle α between 0 and 2π.

On Fig. 4 were also depicted the trajectories (as epicycloid curves) generated by three different points placed on the circular 2D pin profile. First

epicycloid (1 on Fig. 4) is generated by the farthest point of 2D pin profile from O_1 (placed at a distance r_S+r_p), the second epicycloid (2) is generated by the center of the circular 2D pin profile placed at a distance r_S from O_1, the third epicycloid (3) is generated by the closest point from O_1 (placed at a distance r_S-r_p). The left side envelope of this family of circular 2D pin profiles describes as a right border a part of the cycloidal disc 2D profile.

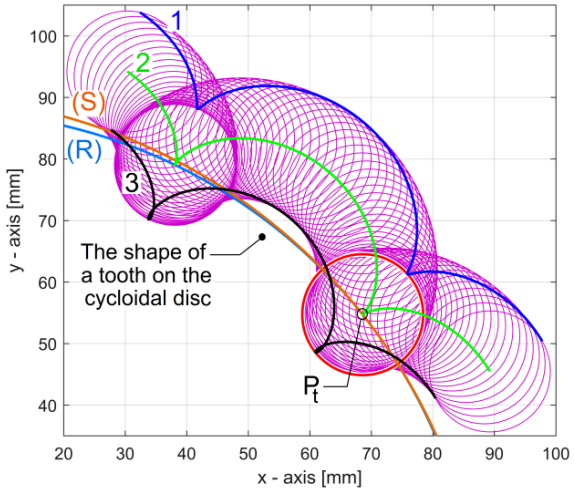


Fig. 5 – Some successive positions of the circular 2D pin profile from Fig. 4 for the incremental variation of the angle α between 2.2π and 6π.

In order to obtain a better conceptual description of a tooth shape on the cycloidal disc, Fig. 4 is rebuilt for a variation α between 2.2π and 6.2π as it is shown in Fig. 5. Here longer epicycloids 1, 2 and 3 are depicted. The rolling circle for the ring gear (S), the rolling circle for the cycloidal disc (R) and their point of tangency P_t were emphasized. Also the shape of a tooth on the cycloidal disc is formally described.

As stated before, there is this strictly relationship $r_S/(r_S-r_R)=Z_S$ from Eq. (7), rewritten as:

$$r_R = r_S \frac{Z_S - 1}{Z_S} \tag{12}$$

That is why, if Fig. 5 is rebuilt for an incremental variation α between 0 and $Z_S \cdot 2 \cdot \pi$, the internal envelope of the successive positions of the circular 2D pin profile should mandatory describe formally the entire 2D cycloidal disc profile, as will be proved here below, in Fig. 6. With $r_{pp}=r_S$ let be a (not mandatory) logical supposition: on the circle with radius r_{pp} (from ring gear) the centers of $2 \cdot Z_S$ tangent circular 2D pin profiles (each one with the same radius r_p) can be placed. Among these $2 \cdot Z_S$ profiles, only Z_S equidistant circular 2D pin profiles are used to describe the positions of Z_S pins as teeth on ring gear. Then

there is an obvious simple geometrical relationship between r_P, r_{pp} and Z_S as it follows:

$$\frac{r_p}{r_{pp}} = \sin\left(\frac{2\pi}{4Z_S}\right) \tag{13}$$

Usually, with an imposed Z_S value (from the CD gear ratio value $-1/(Z_S-1)$), the value of radius r_p is a standard one (especially when the pins are replaced by bearings, in order to reduce the friction with cycloidal disc). It follows that the radius r_{pp} is described from Eq. (13) as:

$$r_{pp} = \frac{r_p}{\sin\left(\frac{\pi}{2Z_S}\right)} \tag{14}$$

With $Z_S=15$ (and $Z_R=14$) and $r_p=5$ *mm*, it follows (from Eq. (14)) that $r_{pp}=47.83386$ *mm*. With $r_S=r_{pp}$ it follows that r_R is described (with Eq. (12)) as $r_R= 44.64493$ *mm*.

If Fig. 5 is rebuilt (only related to the successive positions of the circular 2D pin profile) in these new conditions, for an incremental evolution of the angle α between (at least) 0 and $Z_S \cdot 2\cdot\pi$ (or an incremental variation $\Delta\beta = \Delta\alpha/Z_S = 2\pi/50/Z_S$ of the angle β between 0 and $2\cdot\pi$, according with CR gear ratio formula from Eq. (7)) then the entire 2D cycloidal disc profile is formally obtained, as an internal envelope of these $Z_S \cdot 2\cdot\pi/\Delta\alpha$ position, as it is proved in Fig. 6. Any other evolution of α between 0 and $k\cdot Z_S \cdot 2\cdot\pi$, with the same angular increment, produces exactly the same 2D cycloidal disc profile. On the same Figure are depicted in blue the $Z_S = 15$ circular 2D pin profiles placed on the stator (ring gear). The position of the first pin on the stator is described by $\alpha=0.1885$ *rad*. The entire 2D cycloidal disc profile could be also formally obtained as an internal envelope of the successive positions of these Z_S circular 2D pin profiles (depicted in blue) related on the fixed cycloidal disc, described by the evolution of the angle α only between 0 and $2\cdot\pi$ (with the same increment $\Delta\alpha$).

A first conclusion is available here: it is obvious that the generation of this type of cycloidal disc eliminates any clearance with ring gear (CR works as a zero backlash gear reducer), each pin touch in a single point a teeth on the cycloidal disc, with a sliding friction between. There is a minimum friction in the proximity of the point P_t -the tangential point of circles (S) and (R)- and maximum sliding friction in the diametrically opposed point. This is the main reason to substitute all the Z_S pins with bearings, in order to transform the sliding friction in rolling friction. We should mention that this way (because of bearings) the radial force generated in CR against the cycloidal disc is eliminated. Also, these Z_S bearings play the role of a bearing system for the cycloidal disc motion.

The shape of 2D profile of the active surface on cycloidal discs from literature looks different (as against Fig. 6), because this profile is frequently shifted (with a positive shift *s*). This positive shift *s* implies the decreasing of radius r_S, expressed now as $r_S=r_{pp}-s$.

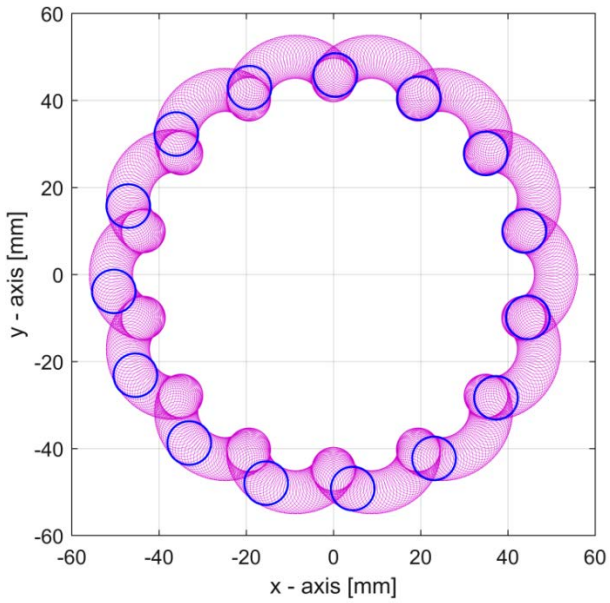


Fig. 6 – The successive positions of a circular 2D pin profile for the incremental variation of the angle α between *0* and $15 \cdot 2\pi$ (in magenta), as border for the 2D cycloidal disc profile. A position of the circular 2D profiles for all the pins placed on the ring gear is depicted in blue, with the first pin placed at $\alpha=0.1885$ *rad*.

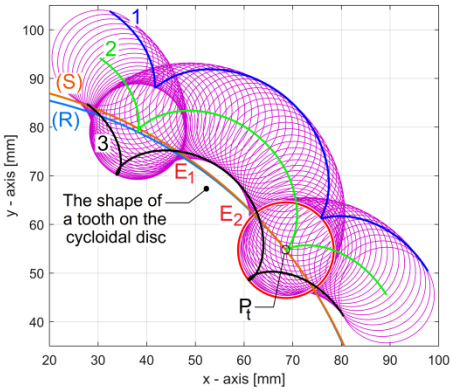


Fig. 7 – The shape of 2D profile of the active surface on cycloidal disc (a copy of Fig. 5, no shifted profile).

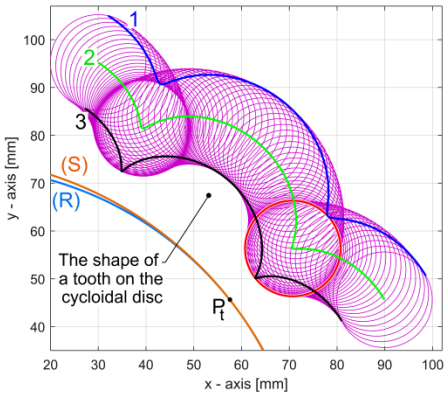


Fig. 8 – The shape of positive shifted 2D profile of the active surface on cycloidal disc (*s=16 mm*).

Usually the shift s is expressed related to r_p using a profile-shifting coefficient c_{ps} (as $s=c_{ps}\cdot r_p$). The Matlab simulation allows of course this positive shift of 2D cycloidal profile. As example, Fig. 8 present the simulation results from Fig. 5 (a copy of this figure is depicted in Fig. 7) but using a diminished radius r_S with $s=16$ *mm* and keeping the relationship between r_S and r_R according with Eq. (12). It is obvious that due to this adequate value of positive shift, the two discontinuities (edges, E_1 and E_2) on each tooth profile indicated in Fig. 7 disappear in Fig. 8. These edges are undesirable mainly because of the risk of contact fatigue.

Figure 9 presents the equivalent of Fig. 6 for cycloidal disc shape description but with a positive shifted ($s=9$ *mm*) of 2D profile in order to remove the edges revealed in Fig. 6. Here $r_p = 5$ *mm* and $r_{pp} =47.83386$ *mm* keep the same values (already used before in Figure 6), only $r_S=38.83386$ *mm* and $r_R= 36.24493$ *mm* are changed (from $r_S=47.83386$ *mm* and $r_R=44.64493$ *mm*) because of the positive shift. As expected, the edges on each tooth were completely eliminated. This is more evident on Fig. 10 which presents a zoom-in detail of Fig. 9 (from the area labelled with A).

It is important to mention that the criteria used in the choosing the right of value for the positive shift s are not considered in this work.

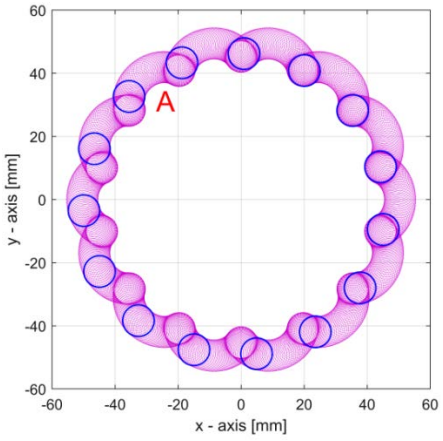


Fig. 9 – The shape of a positive shifted 2D profile of cycloidal disc ($s=9$ *mm*), an improved variant of that generated in Fig. 6.

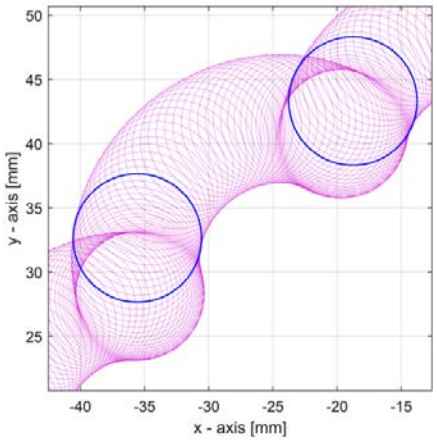


Fig. 10 – A view on a zoom-in detail in area A on Fig. 9. The description of the shape of a tooth on the cycloidal disc (without edges).

It is also important to mention that the shape of the 2D profile of cycloidal disc is furthermore an internal envelope of a family of epicycloid curves generated by some points placed on the pins, towards the inside, under their centers. One of these is the epicycloid 3 in Figs. 7 and 8. This is another reason why the CR rotor is named cycloidal disc.

4. An approach on the description of 2D profile of cycloidal disc

The 2D profile of the cycloidal disc formally defined before should be mandatory described in an available form useful for manufacturing (*e.g.* by CNC contour milling). The most convenient form is the description of the coordinates (as x_{Rf} and y_{Rf}) of all available points on this 2D profile in FCCS system having the origin in O_1. The first challenge is to detect this points, the second is to find out the coordinates of these points.

There are two simple ways to detect these points, as the envelope of the family of circles which describes the successive positions of a pin on the ring gear related to the fixed cycloidal disc. Both ways use a rotary semi straight line (RSSL) with the origin placed in the origin of FCCS, having the angle γ from x-axis.

Here below is described the first way (simpler and faster). A particular position of (RSSL) and the successive positions of the circular 2D pin profile (e. g. the ones described in magenta color on Fig. 6) are described in Fig. 11. The circles which intersect the (RSSL) are selected. The coordinates of the intersection points between (RSSL) and each of these circles are calculated. Only the intersection point located at the smallest distance from the origin O_1 is selected as being certainly placed on the 2D profile of the cycloidal disc. An incremental rotation $\Delta\gamma$ of (RSSL) defines in the same way the next point on cycloidal disc profile. A variation of angle γ between 0 and $2\cdot\pi$ produces a

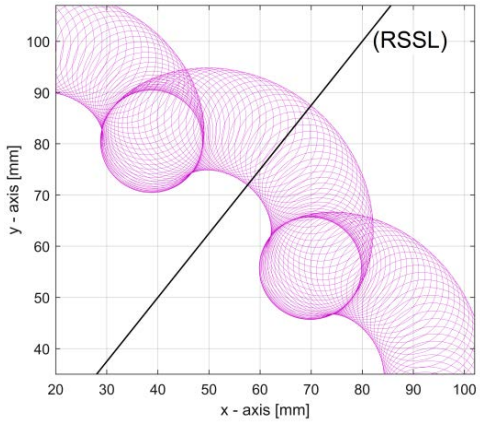


Fig. 11 – A geometrical approach on the determination of 2D cycloidal disc profile (using the simulation from Figs. 5, 7).

complete description of cycloidal disc profile with $2\cdot\pi/\Delta\gamma$ points. If the angular increment $\Delta\gamma$ is small enough (or the number of points involved in the description of cycloidal disc profile is big enough) a line segment between each two successive points on cycloidal disc profile can be considered. This is the

first condition to be met in order to obtain an accurate description of cycloidal disc profile. The second one is to use a small enough angular increments $\Delta\alpha$.

There is a big advantage of this way to find out the description of 2D cycloidal profile: for intersection detection and intersection points coordinate calculus it needs only the coordinates of centers of the circles and the value r_p of a pin radius.

The second way (slower, which involves a longer calculation time) consider each circle as a regular N-sided polygon inscribed in circle, with N as big as possible. Each side is considered to be a line segment. First the line segments which intersect the current position of (RSSL) are selected. Second the coordinates of intersection points are calculated. As previously stated, only the intersection point located at the smallest distance from the origin O_1 is selected as being certainly placed on the 2D profile of the cycloidal disc. Similarly with the first way, each incremental rotation $\Delta\gamma$ of (RSSL) produces the coordinates of a point placed on cycloidal disc profile. Some conditions must be met simultaneously for an accurate description of the cycloidal disc profile: incremental variations $\Delta\alpha$ and $\Delta\gamma$ as small as possible and the number N as high as possible. This second way is privileged in this work.

Figure 12 presents partially the 2D profile of the cycloidal disc formally described in Fig. 11, detected in these last conditions (with $\Delta\alpha=2\pi/50$, $\Delta\gamma=2\pi/3000$ and $N=500$).

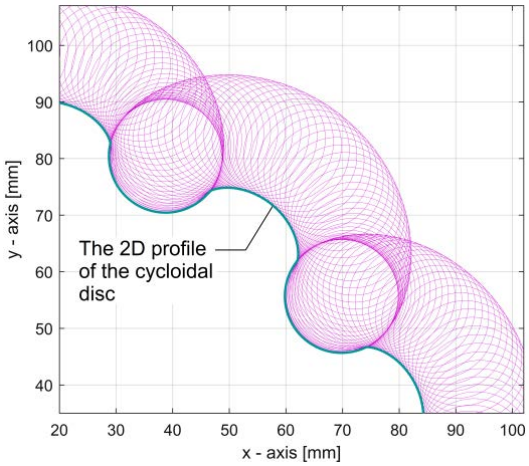


Fig. 12 – A description of the 2D cycloidal disc profile found by analysis of Fig. 11.

Figure 13 presents the 2D profile of the cycloidal disc (with 3000 points, depicted in cyan) formally described before in Fig. 6 (now with $\Delta\alpha=2\pi/200$, $\Delta\gamma=2\pi/3000$ and $N=500$).

There are here 3000 positions (depicted in magenta) of a 2D circular profile of a pin from ring gear. A position of all 15 pins placed on the ring gear

is depicted in white. Figure 14 presents a zoom-in detail on Fig. 13, in area labelled with A.

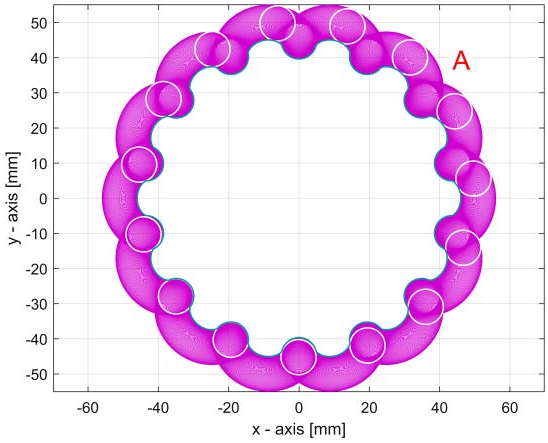


Fig. 13 – The description of the 2D profile of the cycloidal disc found by analysis of Fig. 6.

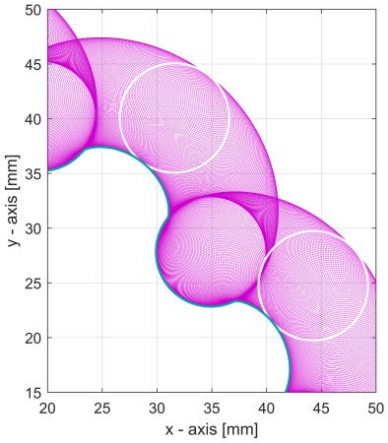


Fig. 14 – A view on a zoom-in detail on Fig. 13 from the area labelled with A.

A better approach of Fig. 13 is given in Fig. 15.

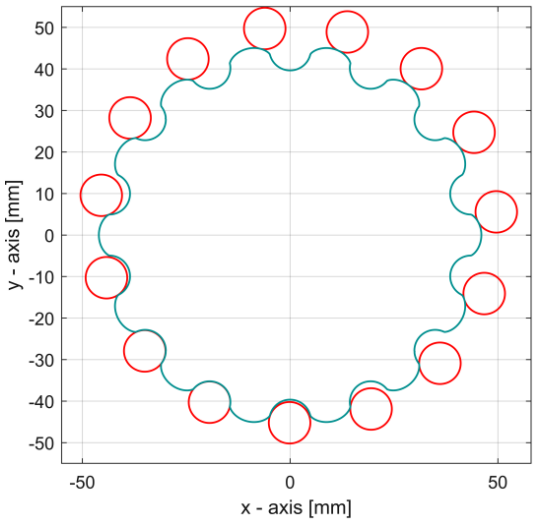


Fig. 15 – The relevant results from Fig. 13 (the 2D profile of the cycloidal disc and the pins from the ring gear).

Here only the 2D profile of the cycloidal disc (in cyan) and a position of all 15 pins placed on ring gear (now in red) are depicted.

A similar analysis (already done in Fig. 13) can be performed in order to find out the description of the positive shifted 2D profile of the cycloidal disc generated in Fig. 9 as it shown in Fig. 16.

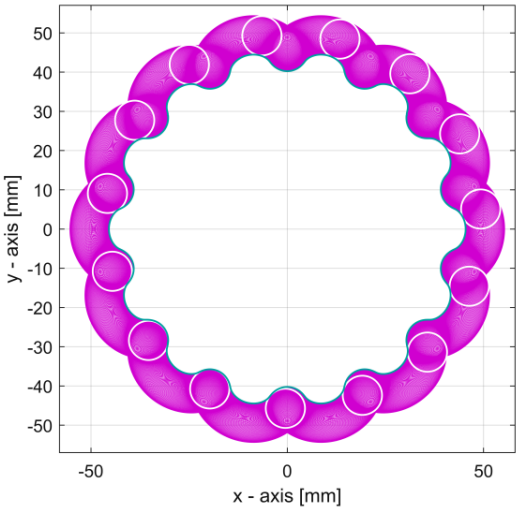


Fig. 16 – The description of the 2D profile of the cycloidal disc (s=9 *mm*), found by analysis of Fig. 9.

Figure 17 depicts only the relevant results from Fig. 16 (the 2D profile of the cycloidal disc and the pins from the ring gear). A zoom-in detail (from area A of Fig. 17 is depicted in Fig. 18.

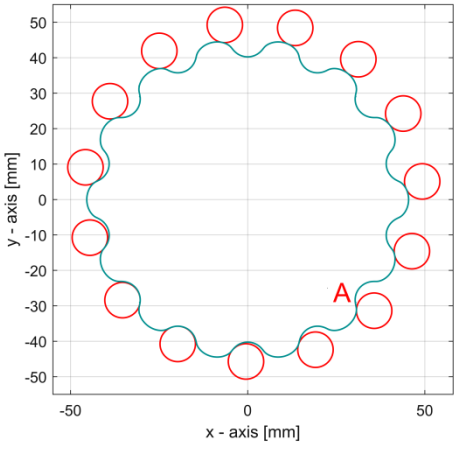


Fig. 17– The relevant results from Fig. 16 (the 2D profile of the cycloidal disc and the pins from the ring gear).

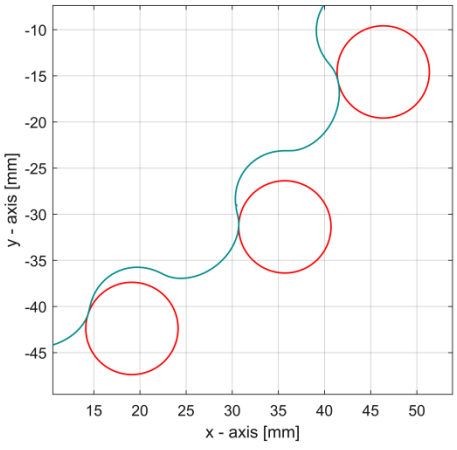


Fig. 18 – A view on a zoom-in detail on Fig. 17 from the area labelled with A.

Some similar studies can be also performed for other pin arrangements on the ring gear (and pin radius as well) or/and other gear ratio values. As example, Fig. 19 presents similarly with Fig. 17 the CR elements (ring pins and cycloidal disc shapes positively shifted) for $Z_S=8$, $r_p=5$, $s=5mm$ and r_{pp} described (slightly different as against Eq. (14)) as:

$$r_{pp} = \frac{4}{5} \cdot \frac{r_p}{\sin\left(\frac{\pi}{2Z_S}\right)} \tag{15}$$

It is well known that in order to eliminate the mass unbalancing at the CR input two cycloidal discs (or two rotors as well) diametrically opposed, (both being placed in internal gear with the same ring gear) are used simultaneously on two different levels as Fig. 20 formally indicates (based on the results from Fig. 19).

The CR keeps the same working principle formally described before in Fig. 1 (and the gear ratio shown in Eq. (1)).

The CR keeps the same working principle formally described before in Fig. 1 (and the gear ratio shown in Eq. (1)). Now two identical cranks (with opposite eccentricity, having the same length and rotation center in O_1 and the same rotary speed $n_{O_2-O_1}$) and two circles (R_1), (R_2) as well are used (one for each cycloidal disc) in gear (rolling) with the same ring gear (the fixed circle (S)). Two different diametrically opposed, tangential and movable points P_{t1}, P_{t2} are now defined (between (R_1) and (S), (R_2) and (S)).

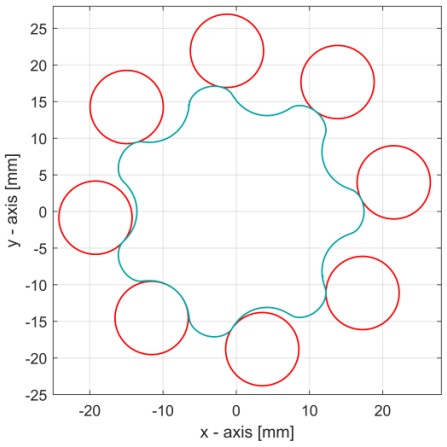


Fig. 19 – The 2D profile of the cycloidal disc and the pins from the ring gear for a CR with $Z_S=8$, $r_p=5$, $s=5mm$ and r_{pp} described by Eq. (15).

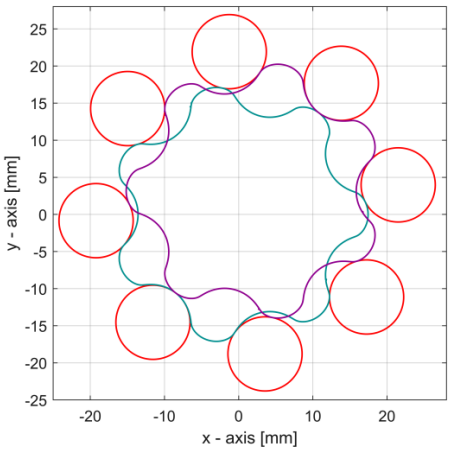


Fig. 20 – A conceptual description of 2D profiles involved in the synthesis of a CR with two cycloidal discs.

It is obviously now that two bearings replace mandatory each pin. Now Z_S bearings play the role of the pins in gear with the cycloidal disc placed on the lower level (*e.g.* that depicted in cyan), the other Z_S bearings play the role of the pins in gear with the cycloidal disc placed on the upper level (that depicted in cyan).

We should mention that the noticeable reduction of friction inside a CR obtained by replacing the pins on ring gear with bearings implies the appearance of an unexpected disadvantage: if the gear ratio is not small enough, the direction of motion transmission in CR (from input to output shaft) is reversible, the braking effect (commonly encountered in other types of reducers, *e.g.* a worm drive) disappears.

5. Some considerations on 2D cycloidal disc profile transfer on 3D CAD model.

The 2D profile of a cycloidal disc can be exported as closed curve (centered in origin of FCCS) in any available CAD software and extruded to obtain a 3D solid in order to obtain the external (active) shape of the cycloidal disc. Any other necessary items for internal shape (*e.g.* the holes necessary for input and output motion) can be made in CAD software. As example, a 3D view of the cycloidal disc having the external shape described by the 2D profile depicted before in Fig. 19 is presented in Fig. 21.

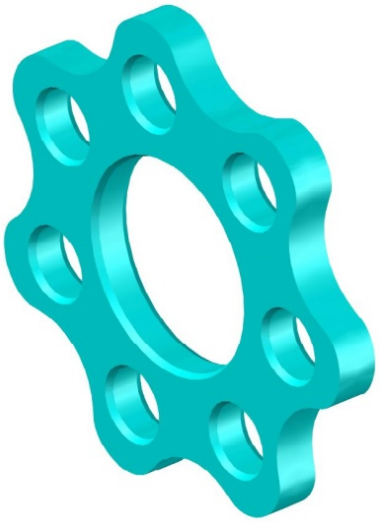


Fig. 21 – A view on a 3D CAD model of the cycloidal disc with the external 2D shape depicted in Fig. 19.

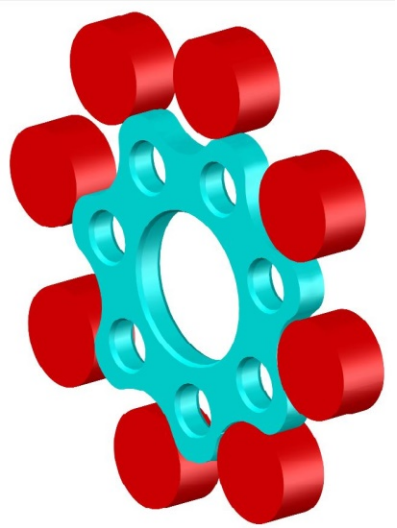


Fig. 22 – A view on a 3D CAD model of the cycloidal disc from Fig. 21, in gearing with the pins formally depicted.

The central hole is used to introduce the input motion in CR (having the rotary speed $n_{O_2-O_1}$ in Fig. 1), the other holes are used to collect the output motion delivered by CR (having the rotary speed n_{R-O_2} in Fig. 1).

Figure 22 presents a view on the 3D CAD model of the cycloidal disc from Fig. 21 in gear with the pins (conceptually depicted in red) placed on the ring gear.

A Computer Aided Manufacture (CAM) software can be used to produce the disc on a CNC machine. The external shape of the cycloidal disc can be easy manufactured by contour milling using the 2D profile generated before.

3. Conclusions

This paper presents in theoretical terms and by simulation some results on the synthesis of 2D profile of cycloidal discs used in cycloidal reducers. The shape of a 2D profile results as an internal envelope of the family of all the equidistant positions of the Z_S cylindrical pins (eventually replaced by bearings) placed on the stator (ring gear) related to the fixed rotor (the cycloidal disc). Firstly this family of equidistant positions was generated by simulation using an adequate theoretical approach, based mainly on Eq. (10) and Eq. (11)) and using some considerations on gear ratio, (number of pins), pins radius, the radius of the circle on which the pins are placed, rolling circles radius, value of shifting profile, etc. Secondly the internal envelope of this family of equidistant positions was detected as 2D closed curve. This closed curve is exactly the 2D profile of a cycloidal disc described in a fixed Cartesian system of coordinates with the center placed in the center of disc as well. Some considerations and comments on the accuracy of the definition of this 2D profile were done.

All the simulations were made with our own computer programs written in Matlab. Despite an enormous amount of calculations, the running time of these programs was reasonable small (tens of seconds).

The 2D profiles of cycloidal discs are useful in CNC manufacturing of these discs (*e.g.* by contour milling) or to generate the external shape of these discs by 3D computer aided design.

The future studies will be focussed on the synthesis of the 2D profile for the stator of a new type of cycloidal reducer having Z_R circular equidistant rotary cylindrical pins placed on the rotor.

REFERENCES

Allotta B., Fiorineschi L., Papini S., Pugi L., Rotini F., Rindi A., *Redesigning the cycloidal drive for innovative applications in machines for smart construction yards*, World Journal of Engineering, **18**, *2*, 302-315 (2021).

Horodincă M., *An approach on simulation of sine gear profile used on cylindrical gears*, Buletinul Institutului Politehnic din Iași, **66 (70)**, *2*, s. Machines Manufacturing, 37-52 (2020).

Horodincă M., Seghedin N.E., *Reduction gear with cylindrical gear wheels and quadrilateral mechanism*, patent RO.*111.610* (B1) /1996.

Huang C.H., Tsai S.J., *A study on loaded tooth contact analysis of a cycloid planetary gear reducer considering friction and bearing roller stiffness*, Journal of Advanced Mechanical Design, Systems, and Manufacturing (Bulletin of the JSME), **11**, *6*, 17-00213 (2017).

Litvin F.L., Feng P.H, *Computerized design and generation of cycloidal gearings*, Mechanism and Machine Theory, **31**, *7*, 891-911 (1996).

Mackic T., Blagojevic M., Babic Z., Kostic N., *Influence of design parameters on cyclo drive efficiency*, Journal of the Balkan Tribological Association, **19**, *4*, 497-507 (2013).

Petrovic N., Blagojevic M, Marjanovic N., Matejic M., *Parametric drawing of a cyclo drive shortened equidistant epitrochoid gear*, Proc. of the 7th International Quality Conference, May 24th, 2013 Center for Quality, Faculty of Engineering, University of Kragujevac, Serbia, 303-308.

Shin J.H., Kwon S.M., *On the lobe profile design in a cycloid reducer using instant velocity center*, Mechanism and Machine Theory, **41**, *5*, 596-616 (2006).

Wang H., Zhao-Yao S., Bo Y., Hang X., *Transmission Performance Analysis of RV Reducers Influenced by Profile Modification and Load*, Applied Sciences, **9**, *19*, 4099 (2019).

UN STUDIU ASUPRA DESCRIERII PROFILELOR 2D ALE ROTORILOR CICLOIDALI FOLOSIȚI ÎN STRUCTURA REDUCTOARELOR CICLOIDALE

(Rezumat)

Lucrarea propune o nouă metodă de obținere a profilelor 2D ale rotorilor cicloidali (din structura reductoarelor cicloidale) în secțiune transversală, drept curbe plane închise, descrise prin coordonatele punctelor lor într-un sistem cartezian bidimensional. Metoda presupune simularea pozițiilor succesive ale statorului (devenit mobil pentru un observator plasat pe rotor) în raport cu rotorul (devenit fix), cu respectarea regulilor angrenării. Curba înfășurată la interior de către pozițiile succesive ale statorului (descris prin dantura acestuia, tipic pentru acest tip de reductoare, sub forma unor cilindri echidistanți pe circumferință, de obicei materializați prin role sau chiar rulmenți) descrie chiar forma bidimensională a profilului transversal al rotorului ciloidal. Lucrarea propune un procedeu de generare a acestor poziții succesive ale statorului și un procedeu de determinare a coordonatelor înfășuratei la interior a acestor poziții, ambele procedee fiind validate prin simulare cu ajutorul unor programe de calculator proprii, scrise pentru mediul Matlab. Profilul 2D de disc cicloidal astfel obținut poate fi transferat și extrudat pe discul (rotorul) cicloidal unde este regăsit pe suprafața exterioară a acestuia (de angrenare cu dantura de pe stator). În lucrare se prezintă un exemplu CAD de model de rotor cicloidal astfel obținut.